Published in Coastal Environment and Water Quality (ed. by Y. J. Xu & V. P. Singh), 47-68.

5

WIND AND TIADAL EFFECTS ON CHEMICAL SPILL IN ST ANDREW BAY SYSTEM

Peter C. Chu and Patrice Pauly
Department of Oceanography, Naval Postgraduate School, Monterey, CA 93943, USA

Steven D. Haeger
Naval Oceanographic Office, Stennis Space Center, MS 39529, USA

Mathew Ward
Applied Science Associates, Inc., 70 Dean Knauss Drive, Narragansett, RI 02882, USA

ABSTRACT

A coupled hydrodynamic-chemical fate model is used to investigate mechanisms for chemical dispersion in the St Andrew Bay system. It is found that the time for the pollutants transporting outward the bay mainly relies on the winds and source location. If the application of the stochastic model somehow handles the wind factor, the release location must be shifted to other places in order to evaluate the relative weight of this factor. Because the flux originating from Gulf of Mexico predominantly flows westward, a release point located between St Andrew Bay and West Bay or even more inside West Bay is likely not to deeply impact East Bay. The pollution will only reach the end of East Bay after 15 days if the pollutant is spilled at point A, which only stands 8km away from the previous spot. As this chemical is not volatile, it does not evaporate and its mass is roughly conserved into the system until its natural decay acts. West Bay is much shallower than St. Andrew Bay, thus the small concentration decrease close to the Gulf entrance involves a large pollutant mass transfer into West Bay.

5.1. INTRODUCTION

St. Andrew Bay system is located in the western part of Florida State close to Pensacola (Fig. 1). It is a long, narrow and rather shallow (water column extends from 4 to 10 m) bay oriented in the northwestern direction. Deer Point Lake located at the northern edge of North Bay, provides the major freshwater inflow into the estuary, along with a number of smaller creeks. Two major passes, East Pass and West Pass, have provided surface water connections via its central part (St Andrew Bay) with the Gulf of Mexico. West Pass was artificially cut in 1934 in Shell Island as the primary navigation channel to the Gulf, while most exchange between the estuary and the Gulf had historically occurred through East Pass. East Pass was recently filled in (1998), however, by the movement of shoreline sediments. Dredging was conducted for reopening the pass in 2001. None of these channel

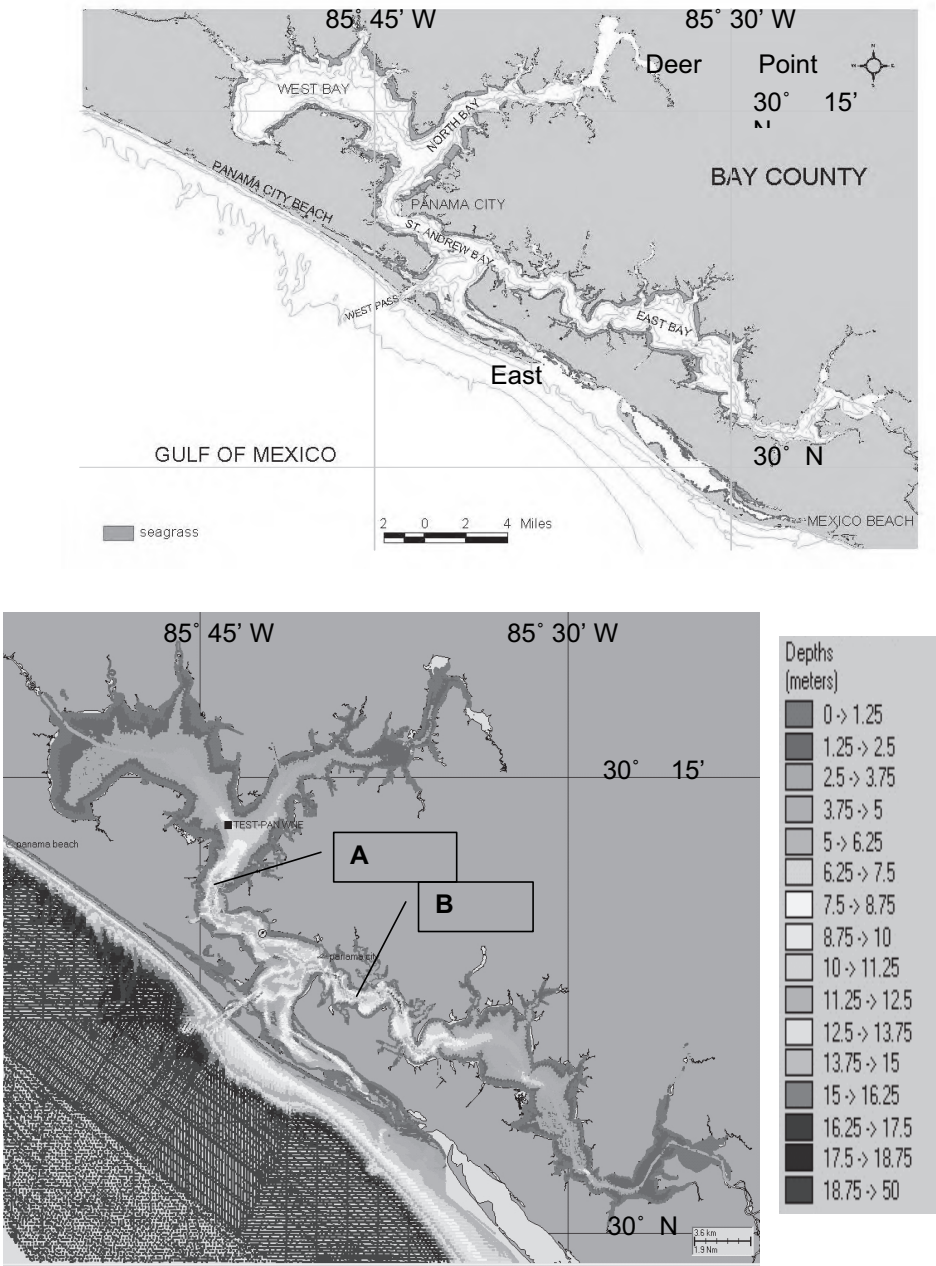

Fig. 1. St. Andrew Bay system geography (upper panel) and bathymetry (lower panel). Note that two points "A" and "B" will be used.

widths exceed 1 km. St Andrew Bay system also links the Intracoastal Waterway on both the very end of the East Bay and the West Bay. The waterway depth is constantly maintained at 4m which causes some water exchanges to occur at these locations.

Drainages into these bays are small and mainly due to groundwater seepage. For example, it is suggested that almost two thirds of the creeks which flow into Deer Point Lake are supposed to be spring fed (Musgrove et al., 1965). Nevertheless their influence can be crucial when modeling the whole system. In terms of estuarine classification, the four basins are generally positive, i.e., drainage inflow exceeds evaporation (Pritchard, 1952) except in St. Andrew bay where neutral conditions, due to its connection with the Gulf, are found (Ichyie and Jones, 1961). The bottom contours are part of the WQMAP geographic information system (GIS) layer and have been provided by NOAA. They depict a 5.2m average depth for St Andrew bay, the mean depth respectively being 2.1, 1.7 and 2m for East, North and West bays.

The shoreline landscape of St Andrew Bay system is known for its high biodiversity, seagrass beds, and its importance as a nursery for coastal fishery resources. Due to its role in fishery production, recreation, and related tourism, it is a key element in the economy of Bay County. Chemical pollutants threaten public health and the environment. In this study, a coupled hydrodynamic-hydrochemical fate model is used to identify the pollutant dispersion patterns. The hydrodynamic sub-model is driven by tides and winds and predicts the velocity field. The hydrochemical model is driven by the velocity field and predicts the chemical spill.

5.2. BACKGROUND

5.2.1. Hydrographic Features

Temperature is rather uniform within the water column through out the bay system with very small vertical variations even in summer (the depth is too shallow for the thermocline to really develop). But its seasonal variability is evident. A five year-study of surface temperature from both inside and outside the bay, conducted using NOAA time series data, shows that the mean temperature varies between 15º C in winter and 30º C in summer. The comparison of these two 5-year-long time series (between 2000 and 2004) portrays a strong zonal sensibility and the difference ranges from 0 during winter time up to 2.5ºC during summer (Fig. 2). The rather shallow bay allows the water column to heat up very quickly; the maximum difference is reached no later than March and lasts almost 9 months.

Salinity, however, presents some zonal features. Close to the Gulf of Mexico connection, the salinity is almost constant within the water column (gradient of 0.17 psu/m) and reaches its highest value (34.3 psu). Its value can drop down to 9 psu at surface nearby with a gradient of 3.3 psu/m (Ichyie, 1961; Blumberg and Kim, 2000). Nethertheless, the 24 h variation of salinity does not correlate closely with variations of the tidal current, specifically away from the bay entrance. The salinity follows the net flows caused by wind driven currents and freshwater inflow events. At last, the hydrographic study conducted by Ichyie proved the water column stability being time independent and mainly subjected to salinity vertical variations (Sverdrup et al, 1942).

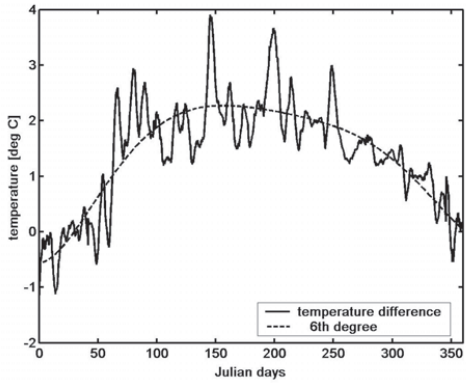

Fig. 2. Temperature difference between St Andrew Bay and Gulf inner shelf.

5.2.2. Tides

The Panama City Beach (30º 12.8'N – 85º 52.7'W) and the St Andrew Bay (30º 09.1'N – 85º 40.0'W) data study shows that according to the form ratio (ratio between diurnal -K1+O1- and semidiurnal -M2+S2-), the tidal constituents are diurnal (ratio greater than 3). High and low water times study show the tidal waves first enter the bay through East Pass (5 minutes difference between East and West Pass) which correlates the general motion of tidal waves. The maximum current is found in the West Pass and can exceed 0.5m/s. It then decreases as low as 0.15m/s at the western end of West Bay. Most of the time, ebb currents duration is longer than flood current duration, mainly due to the effect of drainage, source of a quasi permanent outward current in the upper layer if any (Pritchard, 1952). This process causes "tidal pumping" phenomenon (Fischer et al, 1979).

Compound tides (for ex. M4 ...), often important in shallow water and hence on inner shelves, are generated by the nonlinear interactions of the primary constituents. The long-period tidal constituents are not resolvable in the month-long series, and contributes little (1.1 cm) to the tidal elevation. It is crucial to understand any seasonal effects which may occur on tides. Tidal results from a yearly sea-level time series were compared with those from a monthly subset of the sea-level time series to examine the seasonal effects. Additionally, this provides insight into the effects of unresolved tidal constituents contained in shorter time series. Overall, none of the major diurnal and semidiurnal tidal constituents differed more than 1 cm between the year- and month-long series except K1 constituent which varies significantly. The five main constituents have been computed though 12 successive month-long time series collected in 2004 outside St Andrew Bay and are associated with a 95% confidence interval (Fig. 3). This general trend is consistent with the observations of the last 5 years and denotes the occurrence of a seasonal dependence of both K1 and S2 constituents.

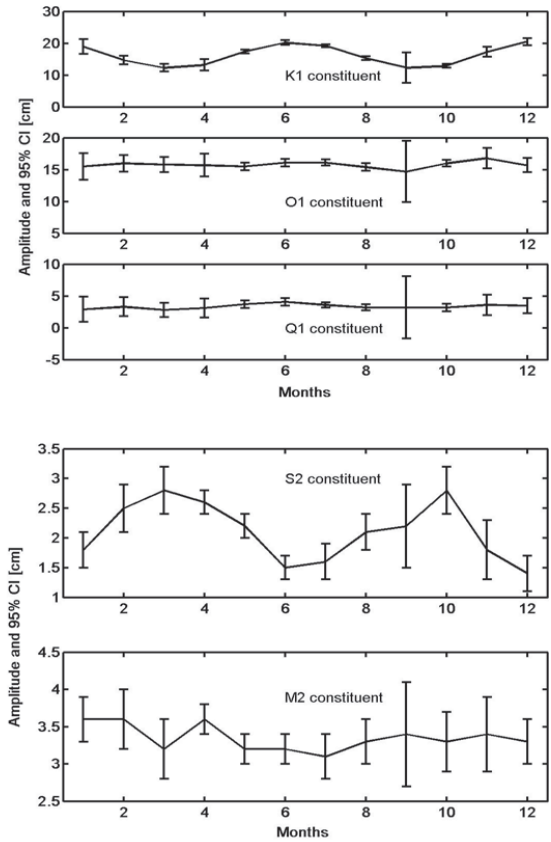

Fig. 3. Seasonal variability of tidal constituents at Panama City Beach.

5.2.3. Fresh Water Supply

Freshwater discharge in the Gulf of Mexico totals approximately 1110 km^3 per year and is dominated by the Mississippi and Atchafalaya rivers, which contribute 55% of this discharge (Solis and Powell, 1999). The extent of the impact of this discharge, both vertically and horizontally, is variable and modulated by discharge rate and processes that disperse the plume, primarily wind stress. The river water accumulates in the inner shelf, forming a low salinity band that supports a persistent baroclinic flow to the south (Atkinson et al., 1983). The mid shelf zone (21-40 m isobaths) is vertically homogeneous during the fall (September, October, November) and winter (December, January, February), due to enhanced wind mixing and decreased runoff. This region undergoes a transition to a vertically stratified state in the spring (March, April, May) and summer (June, July, August) as wind mixing decreases and runoff increases (Atkinson et al., 1983). In addition to runoff, groundwater sources have been shown to be important in the SE region of United States and prevail in the St Andrew bay system.

5.2.4. Alongshore Current and Littoral Transport

The main current affecting the surf zone is the alongshore current created by waves breaking at an angle to the shore. The magnitude of the alongshore current depends on the breaking wave characteristics, breaking angle and local bottom and shore configurations. The alongshore currents are responsible for sand transport along the coast (Chu et al., 2005a). For the study area, the net littoral transport is generally westward as the predominant waves are from the east and is estimated to be about 65,000 cubic yards per year. This estimate seems to be in agreement with the field evidence as indicated by the lack of strong erosion and accretion at the west and east side of the gulf entrance to the St. Andrew Bay (U. S. Army Corps of Engineers, 1971). However, the accumulation of hurricane-induced waves during the 1990's is likely to be responsible for East Pass closure that happened in 1998. Van de Kreeke (1990) showed that a two-inlet system could not be stable for a one-bay system. Even without erosion evidence, one of the inlets has to close. Moreover, Jain et. al (2004) showed that both inlets were actually unstable and hence will request continuous dredging maintenance unless St Andrew bay is enlarged.

All beaches are experiencing erosion, the more severe locating on the northern edge of main entrance channel with a rate of 2.44 m/yr. This process is associated with the construction of St Andrews Inlet in 1934. Similar rates occur along Shell Island and vary from 0.53m/yr in its western part to 1.95 m/yr close to the secondary channel entrance. The lack of construction on Shell Island does not make the eroding process as critical. However, bypass placements of sand have been helping in the stabilization of the shoreline.

These changes are mainly due to extreme weather system hitting the area. Hurricane Eloise in September 1975 caused a 100,000 m^3 beach-dune erosion. Hurricane Opal in October 1995 impacted the area by dredging almost 100,000 m^3 from both beaches and dunes (Bureau of Beaches and Coastal Systems Division). Finally, during hurricane Ivan event in September 2004, beaches alongside Bay County suffered a vertical loss of sand between 1.2 and 1.5 m (Bureau of Beaches and Coastal Systems Division, 2004).

5.2.5. Winds

Located at average latitude of 30º10'N, the St Andrew Bay system is under the influence of rather weak winds (Table 1). The climatology of wind forcing in the Gulf of Mexico exhibits a pattern of seasonal variation. During the fall and winter months (mid-September to mid-February), winds are primarily from the north. In the late spring and summer (from March to July), the northern Gulf of Mexico is dominated by tropical weather with winds mainly southerly. During summer, the influence of the subtropical high (Bermuda High) increases as the frontal zone between subtropical and mid-latitude air masses moves north and out of the Gulf. Weaker pressure gradients and, hence, calmer winds associated with high pressure produce less vigorous wind stress forcing of oceanic or, in particular, shelf

Table 1. Monthly mean wind direction and speed (m/s).

	Jan	Feb	Mar	Apr	May	Jun	Jul	Aug	Sep	Oct	Nov	Dec
Dir.	N	N	SSE	S	S	WSW	WSW	E	ENE	N	N	N
Speed	3.5	3.5	4	3.5	3	3	3	2.5	3	3	3	3.5

circulation. During summer, warm fronts move generally from south to north. The average data collected throughout the last 60 years show very uniform winds.

5.3. HYDRODYNAMIC MODEL

5.3.1. Model Description

The numerical hydrodynamic model implemented for St. Andrew Bay system is a depth-averaged, boundary fitted tidal and residual circulation model known as WQMAP (Muin and Spaulding, 1996; 1997) developed at the Applied Science Associates Inc.. The numerical techniques incorporated in the model are well documented, thus only a summary of the model characteristics is presented. WQMAP is an integrated hydrodynamic and water quality modeling system designed for use within coastal and fresh water environments. This commercial off-the-shelf program was developed by Applied Science Associates, Inc. out of Narragansett, Rhode Island. WQMAP consists of three basic components: a boundary-fitted coordinate grid creation module, a three-dimensional hydrodynamics model, and a water quality or pollutant transport model. These models are executed on a boundary fitted grid system. They can also be operated on any orthogonal curvilinear grid or a rectangular grid, which are special cases of the boundary fitted grid. The model is configured to run in a vertically averaged (barotropic) mode or as a fully three-dimensional (baroclinic) mode. Several assumptions are made in the model formulation, including the hydrostatic (shallow water) approximation, the Boussinesq approximation, and incompressibility. In this study, the 2D version is used.

Most striking feature of WQMAP is its hybrid orthogonal curvilinear-terrain following coordinate system. Let (φ, λ, z) be the latitude, longitude, and height, and (ξ, η, σ) be a hybrid coordinate system with a generalized orthogonal curvilinear coordinate system (ξ, η) in the horizontal and terrain-following σ-coordinate in the vertical. The metric coefficients connecting (ϕ, λ) to (ξ, η) are defined by

$$g_{11} = (\frac{\partial \lambda}{\partial \xi})^2 \cos^2 \phi + (\frac{\partial \varphi}{\partial \xi})^2, \tag{1}$$

$$g_{22} = (\frac{\partial \lambda}{\partial \eta})^2 \cos^2 + (\frac{\partial \varphi}{\partial \eta})^2. \tag{2}$$

The coefficient g_{11} is the metric tensor in ξ-direction and the coefficient g_{22} metric tensor in η-direction. These tensors permit the model to transform the user defined boundary fitted grid to a numerical grid employed for spatial discretization utilized in an Arakawa *C* Grid.

Let (ζ, *H*) be the surface elevation and bathymetry. $D = H + \zeta$, is the total water depth. The σ - and z-coordinates are connected by

$$\sigma = \frac{z + H}{\zeta + H}, \tag{3}$$

which makes $\sigma = 1$ for the ocean surface and $\sigma = 0$ for the ocean bottom.

The 2D WQMAP represents a depth-averaged shallow-water system (similar to Wang et al., 1998). Let (*U*, *V*) be the vertically averaged velocity components in (ξ, η) directions. The momentum equations for (*U*, *V*) are given by

$$\frac{\partial UD}{\partial t} + \frac{1}{\sqrt{g_{11}g_{22}}}\left[\frac{\partial\left(U^2 D\sqrt{g_{22}}\right)}{\partial\xi} + \frac{\partial\left(UVD\sqrt{g_{11}}\right)}{\partial\eta} + UVD\frac{\partial\left(\sqrt{g_{11}}\right)}{\partial\eta} - V^2\frac{\partial\left(\sqrt{g_{22}}\right)}{\partial\xi}\right] - fDV$$
$$= -\frac{gD}{R\sqrt{g_{11}}}\left[\frac{\partial\zeta}{\partial\xi} + \frac{D}{\rho_0}\int_{-1}^{0}\int_{\sigma}^{0}\left(\frac{\partial\rho}{\partial\xi} - \frac{\sigma}{D}\frac{\partial D}{\partial\xi}\frac{\partial\rho}{\partial\sigma}\right)d\sigma\right] + \frac{1}{\rho_0}\left(\tau_\xi^w - \tau_\xi^b\right) + A_h D\nabla^2 U, \tag{4}$$

$$\frac{\partial VD}{\partial t} + \frac{1}{\sqrt{g_{11}g_{22}}}\left[\frac{\partial\left(UVD\sqrt{g_{22}}\right)}{\partial\xi} + \frac{\partial\left(V^2 D\sqrt{g_{11}}\right)}{\partial\eta} + UVD\frac{\partial\left(\sqrt{g_{22}}\right)}{\partial\xi} - U^2\frac{\partial\left(\sqrt{g_{11}}\right)}{\partial\eta}\right] + fDV$$
$$= -\frac{gD}{R\sqrt{g_{22}}}\left[\frac{\partial\zeta}{\partial\eta} + \frac{D}{\rho_0}\int_{-1}^{0}\int_{\sigma}^{0}\left(\frac{\partial\rho}{\partial\eta} - \frac{\sigma}{D}\frac{\partial D}{\partial\eta}\frac{\partial\rho}{\partial\sigma}\right)d\sigma\right] + \frac{1}{\rho_0}\left(\tau_\eta^w - \tau_\eta^b\right) + A_h D\nabla^2 V. \tag{5}$$

The continuity equation is represented by

$$R\sqrt{g_{11}g_{22}}\frac{\partial\zeta}{\partial t} + \frac{\partial\left(UD\sqrt{g_{22}}\right)}{\partial\xi} + \frac{\partial\left(VD\sqrt{g_{11}}\right)}{\partial\eta} = 0. \tag{6}$$

Here, *R* is the earth radius; ρ_0 (= 1025 kg m^{-3}) is the characteristic density for the seawater; *f* is the Coriolis parameter; *g* is the acceleration due to gravity; A_h is the horizontal eddy viscosity; $(\tau_\xi^w, \tau_\eta^w)$ are the wind stress; and $(\tau_\xi^b, \tau_\eta^b)$ are the bottom stress. As with any depth-averaged model, it is implicitly assumed that velocity and density are nearly constant over the water column. However, horizontal density gradients are treated explicitly in the momentum equations. As we mentioned in Section 2 that the freshwater flow and surface winds in the bay are low. The currents in St. Andrew Bay system are predominately produced by tides. Thus, the horizontal density gradient can be neglected in short-term prediction.

5.3.2. Model Configuration

The results from Blumberg and Kim (2000) being considered, in this particular study, we ran the model with a rectangular grid in its baroclinic mode. The number of layers was set to 10, every layer representing one tenth of the averaged water column depth within every cell. The model is rather sensitive to bathymetry changes occurring between two nearby cells. To avoid it to blow up, smoothing passes were to be applied on top of the grid averaging and each cell was assigned a minimum 2m-depth to avoid large computational flux increase. This process led to significant depth changes over the whole bay. As the model conserves the total mass, the resulting speeds computed in the different cases correspond to the smoothed depths. A careful attention must so be taken if these values have to be used for operational applications. A similar model popularly used in the coastal oceanographic community is the Princeton Ocean Model (POM). Chu et al. (2001, 2005b) show the capability of POM for littoral prediction.

Since the temperature is well mixed through the water column, we considered it as being constant in order to ease the computational effort. The modal choice is obvious and will not be discussed; the choice of a rectangular grid was driven by computational time restriction. For satisfying the CFL condition, the time step had to be set to 0.1 minute, and hence each run was requesting 17 hours.

5.3.3. Lateral Boundary Conditions

Overall, there are 15 sources of freshwater that are used as part of the model forcing (Fig. 4). The major source of freshwater to the bay is Deer Point Lake. Daily-based flow rates were calculated using measured weir heights at the dam itself. The long-term average flow is 27m^3/s (Musgrove et al., 1965). Freshwater also enters the bay at many other locations. Unfortunately, these sources are largely ungauged even through the flows are often substantial, especially during times of intense precipitation. Table 2 represents the volume transport estimated by Ichyie (2000). Nevertheless these data are not as crucial, and thereby as accurate as they would have been for mass transfer computation. The effect of their fluctuation is, in this study, what is sought.

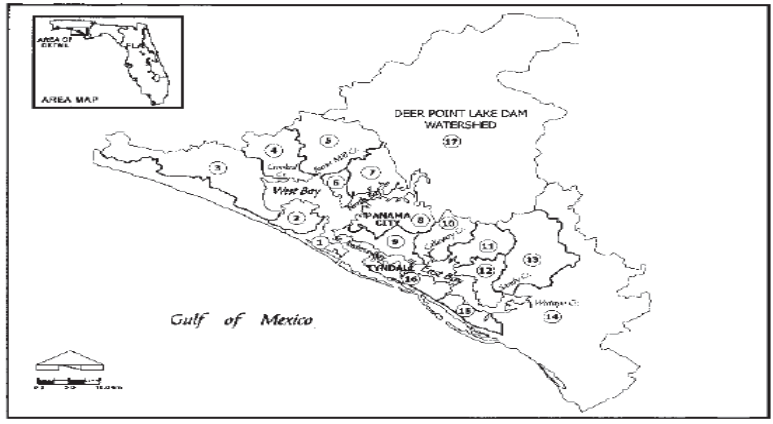

Fig. 4. St Andrew Bay drainage sub-basins (30˚ N - 85˚ 30' W).

Table 2. Calculated Mean volume transport calculated by Ichyie (2000).

Sub-basin	1	2	3	4	5	6	7	8	9	10	11	12	13	14	15	16	17
m^3/s	0.5	0.8	-	1.3	1.4	0.4	1.4	1.7	1.0	1.2	1.2	1.0	3.8	-	0.7	0.9	38.1

Despite the seasonal fluctuation of temperature, we ran the different configuration setting a constant 21˚C temperature value. As the temperature is uniform over the water column, its influence on density distribution is negligible. Forcing the fresh water temperature to the same value has probably introduced the larger error. The different boundaries -West Bay, Gulf entrances and East Bay- were given salinity values -22, 35, 20 psu respectively- in agreement with measurements collected by Blumberg and Kim (2000).

Finally, the rivers cells were forced with pure fresh water which remains questionable as water enters the system through seepage.

5.3.4. Wind Forcing

The wind files were also collected at Panama City Beach and have been applied unmodified and uniformly over the whole domain. The station provides data hourly in standard weather conditions and increases the sampling to every 6 minutes when extreme weather does occur. WQMAP automatically manages the sampling differences.

5.3.5. Tidal Forcing

Data were collected at Panama City Beach where NOAA's National Ocean Service maintains a station providing among others water elevation in meters above MLLW (Mean Lower Low Water) every 6 (or 60) minutes. As we considered the flow entered the bay through two passes the evolution of each tidal constituent was examined as they propagate from East Pass onto West Pass on the continental shelf. The distance separating the two channels is 11.5 km. As a result, the phase shifts were of the order of the degree (1.1º for diurnal constituents and 2.5º for semi-diurnal constituents) and corresponded to a 5 minute-time lag. Moreover, the slight difference on the bathymetry in front of both entrances did not involve a large magnitude difference (0.1% for semi-diurnal constituents - K1 or O1- up to 2% for shallow water constituent – M4 – which only contributes little (1.1cm). At the end, these modifications were ignored. At last, even if the time series used at both locations were issued from Panama City Beach, 30km north of East Pass, we would not have had to correct them because the results from these series had not to be compared with any measured data set. However, NOAA/NOS does not maintain gauge at the three open boundary locations and therefore the elevation time series were got using Wxtide32 software (also called Tides and Currents) which is a free tool providing pure tidal elevation all around the world. Table 3 represents from left to right the Fourier decomposition of elevation gauge time series collected at NOAA station on Panama City Beach, the tidal constituents used by NOAA for predicting tides at Panama City Beach and the Fourier decomposition of tide predictions from Wxtide32 software. Numbers in parenthesis represents the 95% confidence interval for the computed values.

Table 3. NOAA tidal table for Panama City beach.

	Collected data study		NOAA prediction data		Tide and current software	
	Amplitude (cm)	Phase (deg)	Amplitude (cm)	Phase (deg)	Amplitude (cm)	Phase (deg)
K1	15.89 (0.3)	296.2 (1)	14.5	286.7	15.53 (0.1)	313.9 (1)
O1	15.84 (0.3)	284.8 (1)	14.1	284.5	15.95 (0.1)	302.3 (1)
Q1	3.4 (0.3)	270.7 (5.5)	3.1	273.4	3.5 (0.1)	295.0 (4)
M2	3.4 (0.1)	287.4 (1.5)	3.4	277.1	2.3 (0.1)	329.5 (1)
S2	2.0 (0.1)	303.1 (2.5)	2.0	274.5	0.7 (0.1)	325.2 (3)
Form Ratio	5.90		5.30		10.50	

The major difference between the data from Tides and Current software and NOAA data lies in the semi-diurnal constituents which seem to be underweighted. However the resulting error remains low, being considered the low amplitudes of both M2 and S2. A comparison of both NOAA gauge and Wxtide32 software time series (Fig. 5a) shows that differences are larger during spring tides. Finally, as NOAA could not provide time series for the lateral open boundaries, they were forced with Tides and Currents data. To be consistent, we also decided to force the Gulf open boundaries with time series provided by this software.

The residual elevation (Fig. 5b) composed from storm surge, wind-induced waves and wave setup was obtained from the NOAA gauge measurements after filtering the tidal elevation out. The times series depicts a rather uniform shape, except during the hurricane event in September. The residuals provide an average 7.7 cm setup, its standard deviation being 13.6 cm. It is to notice that the hurricane event does not impact much the statistics. When disregarding it, the mean drops to 7.3 cm and the standard deviation to 11.8 cm. These residuals were put on top of the tidal elevation when forcing the last run Gulf open boundaries.

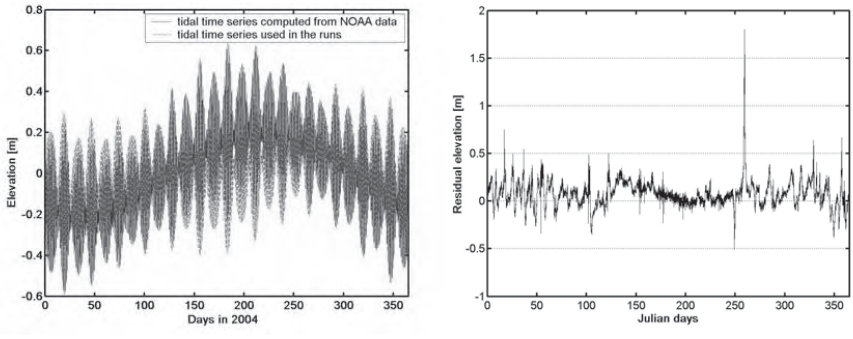

(a) (b)

Fig. 5. Time series of surface elevation: (a) comparison between NOAA (solid curve) and Wxtide32 datasets (dashed curve), and (b) residual from storm surge, wind-induced waves and wave setup.

5.4. CHEMICAL SPILL MODEL

5.4.1. Model Description

A chemical spill model, called CHEMMAP and developed at developed at the Applied Science Associates Inc., is used to predict the trajectory and fate of floating, sinking, evaporating, soluble and insoluble chemicals and product mixtures. It estimates the distribution of chemical elements (as mass and concentrations) on the surface, in the water column and in the sediments. The model is 3D, separately tracking surface slicks, entrained droplets or particles of pure chemical, chemical adsorbed to suspended particulates, and dissolved chemical (McCay and Isaji, 2002). The CHEMMAP model is used to predict the propagation of chemicals.

CHEMMAP can be either run as a certain scenario with tidal and wind forcing or in stochastic mode to estimate the probable distribution and concentrations resulting from hypothetical spills. In this study, CHEMMAP was used to predict the chemical spill in San

Diego Bay. Therefore, the physical characteristics (such as velocity, temperature, salinity) of this tidally dominated bay are simulated using WQMAP. It incorporates a number of model components including simulation of the initial release for surface and subsurface spills, slick spreading, transport of floating, dissolved and particulate materials, evaporation and volatilization, dissolution and adsorption, sedimentation and degradation. It uses physical and chemical properties such as density, viscosity, vapor pressure, surface tension, water solubility, environmental degradation rates, and adsorbed/dissolved partitioning coefficients. The Stoke's Law is used to calculate vertical velocities. Furthermore, its approach towards propagation is Langrangian. The outputs of the model include the trajectories, and concentrations. More specifically, it is possible to see the swept area by a floating chemical, as well as the total, absorbed, dissolved and particulate concentration in both the water column and the sediments. The most important is that it is then possible to determine the range of distances and directions of the contamination caused from the spill at a particular location. The database encloses all the physical/chemical properties required for simulating transport and fate of the spilled material. CHEMAP uses either the Chemical Abstract System (CAS) registry number or the UN number to reference each chemical. The chemical state can be defined as solid, liquid or gas, dissolved or not in aqueous solution or in solvent. As chemical properties do vary with temperature, there all referred to their value at 25˚C.

5.4.2. Model Initialization

The model is initialized for the spilled mass at the location and depth of the release. The state and solubility are the primary determining factors for the initialization algorithm. If the chemical is highly soluble in water and is either a pure chemical (e.g., the benzene scenario) or dissolved in water (e.g., the methanol scenario), the chemical mass is initialized in the water column in the dissolved state and in a user-defined initial volume. For insoluble or semi-soluble gases released underwater (e.g., the naphthalene gas scenario), the spilled mass is initialized in the water column at the release depth in a user-defined plume volume, as bubbles. The median particle size is characterized by a user-defined diameter (McCay and Isaji, 2002).

For the state where the chemical of interest is both adsorbed to particles and dissolved in the water phase of the bulk liquid (e.g. our ammonia liquefied gas scenario), dissolved mass is also initialized in the initial plume volume. The mass of chemical spilled is corrected from the bulk spill volume using the appropriate density and concentration data from the database (McCay and Isaji, 2002).

Chemical mass is transported in three-dimensional space and time, by surface wind drift, other currents, and vertical movement in accordance with buoyancy and dispersion. The model simulates adsorption onto suspended sediment, resulting in sedimentation of material. Stoke's Law is used to compute the vertical velocity of pure chemical particles or suspended sediment with adsorbed chemical. If rise or settling velocity overcomes turbulent mixing, the particles are assumed to float or settle to the bottom. Settled particles may later re-suspend (assumed to occur above 20 cm/s current speed). Wind-driven current (drift) in the surface water layer (down to 5m) is calculated within the fates model, based on hourly wind speed and direction data. Surface wind drift of oil has been observed in the field to be 1-6% of wind speed in the direction of 0-30 degrees to the right (in the northern hemisphere) of the down-wind direction (Youssef and Spaulding, 1993). The user may also specify the wind drift speed and angle (McCay and Isaji, 2002).

CHEMMAP simulates degradation, volatilization, evaporation, dissolution, entrainment and spreading. More specifically, spreading is simulated using the Fay algorithm (Fay, 1971). Entrainment is modeled as for oil (Delvigne and Sweeney, 1988). Surface floating chemicals interaction with shorelines is simulated based on the algorithms developed for oil spills. The dissolution rate of pure chemicals is a function of solubility using a first order constant rate equation. The dissolved chemical in the water column is assumed to adsorb to particulate matter in accordance with the equilibrium partitioning theory (DiToro et al., 1991). Evaporation is modeled following the theory that the rate of mass flux to the atmosphere increases with vapor pressure, temperature, wind speed and surface area (Mackay and Matsugu, 1973). Volatilization from the water column is calculated from the chemical's vapor pressure and solubility (Lyman et al., 1982). Degradation is estimated assuming a constant rate of "decay" specific to the environment where the mass exists (i.e., atmosphere, water column or sediment).

The spilled chemical is modeled using the Lagrangian approach. At each time step, phase transfer rates (evaporation, dissolution, volatilization, and entrainment) are calculated and a proportionate percentage of the spillets are transferred to the new phase (McCay and Isaji, 2002).

The currents in the surface water layer (surface drift currents) are calculated with hourly wind field. The surface drift currents have the magnitude ranging between 1 and 6% of the wind speed and are in a direction 0-30˚ to the right (in northern hemisphere) of the down-wind direction. In this study, the horizontal turbulent diffusion coefficient ranges between 1 and 10m^2/s and its value was set to 1 m^2/s in the different cases. The vertical turbulent diffusion coefficient ranges from 10^{-5} (for stratified ocean) to 10^{-3} m^2/s (for well mixed ocean). The chemical is modeled using a Lagrangian approach in which spillets are tracked in both space and time. All the phase transfer rates are computed at each time step. This type of model is frequently used to trace back harmful substances to their sources and constitutes a valuable tool in the identification of environmental polluters.

5.5. CHEMICAL POLLUTANT- ETHYLENE GLYCOL

The choice of the chemicals used in this study is based on chemical/physical properties and toxicity data and are contained in a database compiled from published literature sources. Since several properties vary with temperature, the chemical data are for an initial temperature of 25^{o}C. The model corrects these parameters to the ambient temperature for the spill incident. The algorithms for changing viscosity and vapor pressure to ambient temperature. For pure chemical processes, the increase per 10^{o}C is assumed to be a factor of 2. For biological processes (e.g., degradation rates), the increase in rate per increase of 10^{o}C is assumed to be a factor of 3 (McCay and Isaji, 2002). In this paper, an chemical pollutant, ethylene glycol, is selected as an example for the study.

Ethylene glycol (OH-CH_2-CH_2-OH) is a non volatile, soluble sinker, its density being 1.1132 $\times 10^3$ kg/m^3. It is referenced as CAS 107-21-1 or UN 8027. Ethylene glycol is a clear, colorless, slightly syrupy liquid at room temperature. It is odorless but has a sweet taste. It is used to make antifreeze and de-icing solutions for cars, airplanes, and boats; to make polyester compounds; and as solvent in the paint and plastics industries. Ethylene glycol is also an ingredient in photographic developing solutions, hydraulic brake fluids and in inks used in stamp pads, ballpoint pens, and print shops.

With eating or drinking very large amounts, ethylene glycol can result in death, while large amounts can result in nausea, convulsions, slurred speech, disorientation, and heart and kidney problems. Female animals that ate large amounts of ethylene glycol had babies with birth defects, while male animals had reduced sperm counts. However, these effects were seen at very high levels and would not be expected in people exposed to lower levels at hazardous waste sites. Ethylene glycol affects the body's chemistry by increasing the amount of acid, resulting in metabolic problems. Similar to ethylene glycol, propylene glycol increases the amount of acid in the body. However, larger amounts of propylene glycol are needed to cause this effect. Its primary hazard is the threat to the environment. Immediate steps should be taken to limit its spread to the environment. Since it is a liquid it can easily penetrate the soil and contaminate groundwater and nearby streams. The EPA has set a drinking water guideline for ethylene glycol of 7,000 μg in a liter of water for an adult. The American Conference of Governmental Industrial Hygienists (ACGIH) recommends a maximum level of 127 milligrams of ethylene glycol per cubic meter of air (127 mg/m³) for a 15-minute exposure.

5.6. CHEMICAL SPILL PATTERNS

In all cases, 10 tons of the aforementioned chemical constituent is released within 10 hours with an original plume thickness of 0.5m. The choice of the date did not respond to any particular need. The release locations, however, are selected in order to identify the tidal pumping effect and minimize the vertical mixing process.

5.6.1. Control Run

The chemicals are released at the mouth of the bay (30˚ 08’ 45.5”N, 85˚ 40’ 46.8”W) 12 am on June 1st. The observed wind vector field is shown in Fig. 6a. We analyze differences between surface and bottom release. As ethylene glycol is not volatile, the evaporation process is weak. Because of the tidal pumping, the chemical dilutes far away from its source in both West Bay and East Bay directions (Fig. 6b). Even if this location is closer to East Bay, it essentially diffuses westward accordingly with the mean winds (from 155˚ at 4 m/s) whereas flow tends to push the water eastward. The maximum dissolved concentration rarely exceeds 1mg/m^3 beyond 85˚35’ toward East Bay and occurs between 4 and 10 days after the release. The same peak reaches a position as far as 8.5km south west of West Pass on the inner shelf 4 days after the release. A maximum concentration of 32000 mg/m^3 is obtained 1 hour after the release started (Fig. 7a). Figure 7b shows that the ethylene glycol is immediately mixed into the water column. Its decreasing rate is 0.3024 per day at 25˚C and after 3 weeks ethylene glycol has disappeared from the bay.

It is however difficult to correlate the signal between two different locations as the plume goes back and forth with tides and as the concentration depends upon the depth at each location. As it propagates westward from the release point to the end of West Bay, the shape of the signal varies significantly as shown in Fig. 8. We can also notice that, the shape smoothes with time (only the largest peak can be tracked) but when the depth is shallow enough, we detect again higher peaks which were present nearby the release location. It is clear from these plots that the water depth influences the dissolved concentration between the last two locations (the depth decreases from 10 to 2m). The concentration naturally decreases as we move away from the source. Fig. 8d shows the

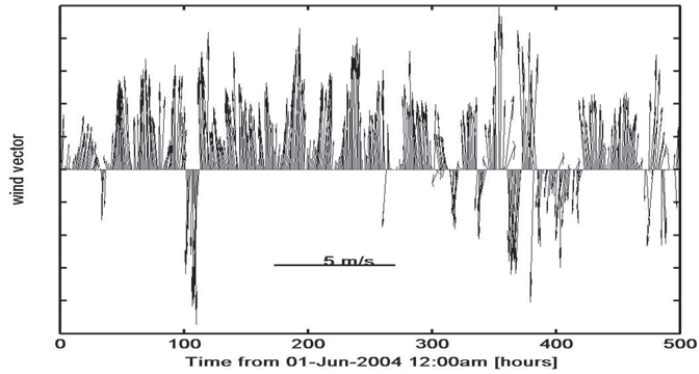

(a)

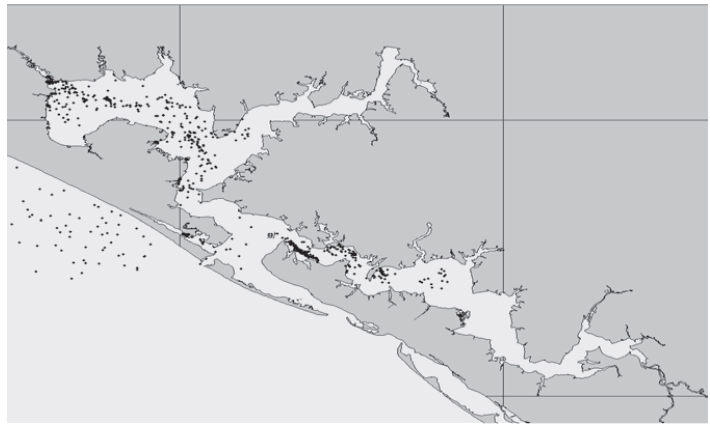

(b)

Fig. 6. (a) Wind field over the domain between the 01-Jun-2004 12:00am and the 21-Jun-2004 11:00 pm, and (b) spillet distribution at 3 weeks after releasing from the bay mouth.

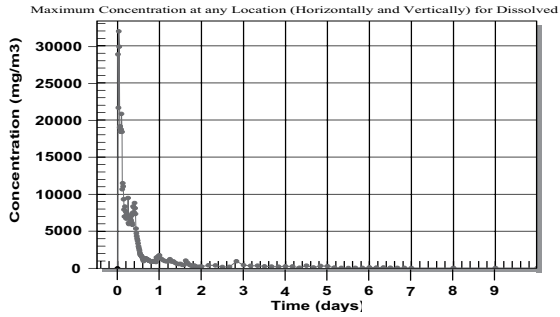

(a)

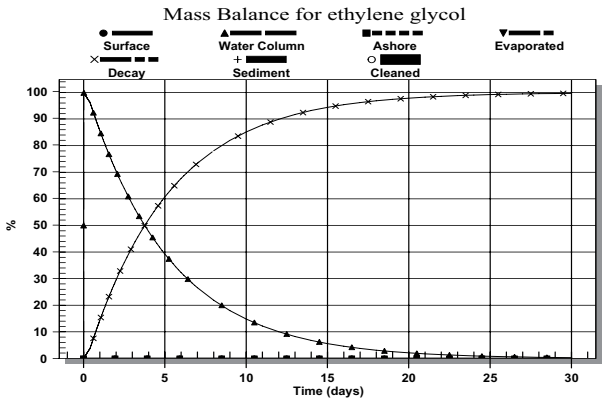

(b)

Fig. 7. (a) Temporally varying maximum concentration, and (b) mass balance for dissolved ethylene glycol at the west pass of the inner shelf.

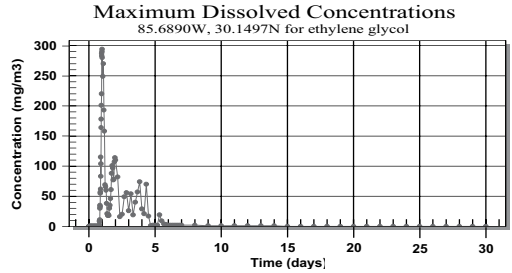

(a)

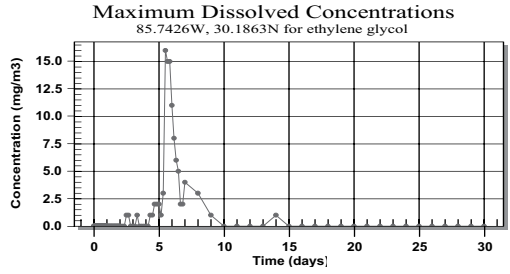

(b)

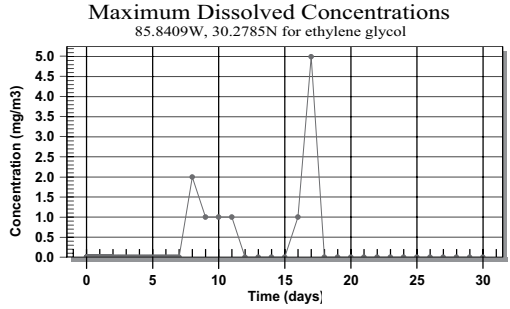

(c)

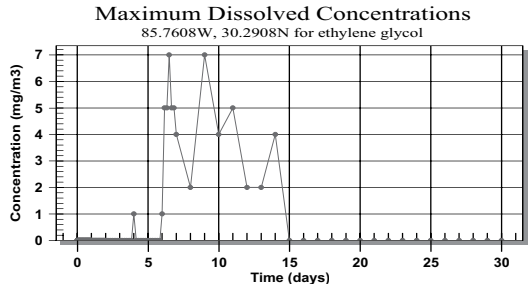

(d)

Fig. 8. Temporally varying maximum concentration at (a) St Andrew Bay, (b) location-A, (c) West Bay open boundary, and (d) northern West Bay.

enhancement of the effects a semi enclosed small creek can produce. With southeastern winds, the chemical piles up in the northern part of West Bay where it remains and accumulates until being diluted into West Bay by changing wind conditions. We can therefore find lumps of pollutant in very small areas which can more severely impact the environment.

5.6.2. Effect of Winds

If the tidal influence in the spreading of the plume can be viewed during the simulation, the impact of the wind is less obvious. Two cases are designed to show the wind effect: (1) reversing wind direction and (2) eliminating wind. When the simulation was done without wind, most of the pollution remained contained between points A and B defined in the previous chapters during the first two weeks (the 15th of June corresponds to the highest tidal range after the release). After that period, a large part of the chemical diffuses into West Bay (Fig. 9a). As the pollutant transits within the mean flow in West Bay, it seems to pile up in different places in East Bay. This does not reflect the truth but only the situation at that particular snapshot. When the wind field is reversed, it is not surprising that the pollutants mainly diffuse eastward (the average wind now blows from WNW at 4 m/s) and outward the bay system (Fig. 9b).

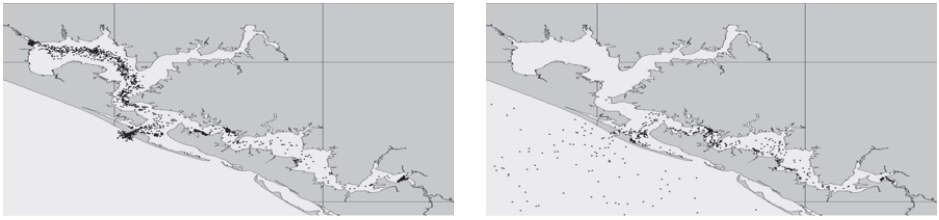

(a) **(b)**

Fig. 9. Spillet distribution at 3 weeks after releasing from the bay mouth with (a) no wind, and (b) wind reversal.

5.6.3. Effect of Release Time

The stochastic model is used to feature with 50 randomized dates of release taken between the 1st of June and 31st of August. Fig. 10a represents the run number of the worst case scenario for each cell (each run is featured with different release date, then different wind and current data but same location and same amount of chemical). The worst case scenario is defined for giving the maximum value encountered at each cell during all the runs. To each tone of grey correspond 5 consecutive runs (even if they are not related to each other).

Figure 10b shows a severe case with a maximum dissolved concentration and two major features. First, the pollutant predominantly diffuses westward which correlates the averaged wind encountered during this period of the year. Second, the pollutant tends to concentrate in shallow motionless waters on the edges of West and East Bay. Note that the two patches of lower concentration in St Andrew Bay correspond to the deepest locations of the bay.

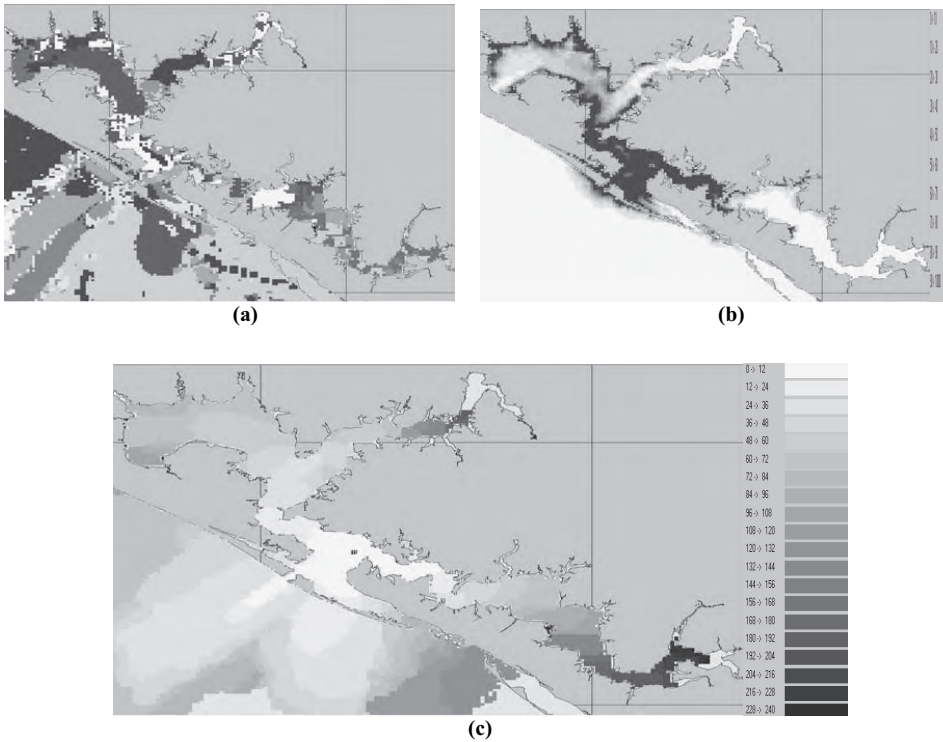

Fig.10. Worst case scenario: (a) run numbers, (b) maximum dissolved concentration (mg/m^3), and (c) minimum time (hours) to exceed threshold.

Therefore, defining the probability a threshold to be overshoot at each grid cell is important. This threshold represents a short term exposure limit (STEL) or an immediately dangerous for life or health (IDLH) limit. The model provides such a probability being given in percentage of runs during which this threshold has been exceeded. If we only consider the possibility of the bay system to be polluted (threshold is given a 0-value), then this percentage is 100% for the whole bay except in the northern part of North Bay and the eastern one of East Bay where probability never drops under 50%. The knowledge of such a probability is vital for deciding the deployment of antipollution devices. But of even furthest importance is the time given before this value can be reached. Fig. 10c then represents the minimum time requested for exceeding the threshold at each grid cell. Hence, for that particular release location, all St Andrew Bay will be polluted within 12 hours, within 24 hours the pollution will extend from point A to the first third of East Bay. It will last over 3 days for the pollutant to reach West Bay open boundary and 10 days for East Bay's.

5.6.4. Effect of Spill Location

It is obvious that the time for the pollutants transporting outward the bay mainly relies on the winds and source location. If the application of the stochastic model somehow handles

the wind factor, the release location must be shifted to other places in order to evaluate the relative weight of this factor. We then applied the same concept to 4 different sites, point A, point B, the center of East Bay and the center of West bay which were supposed to depict different pollutant propagation features accordingly with the hydrodynamic model results.

Because the flux originating from Gulf of Mexico predominantly flows westward, a release point located between St Andrew Bay and West Bay or even more inside West Bay is likely not to deeply impact East Bay. The pollution will only reach the end of East Bay after 15 days if the pollutant is spilled at point A, which only stands 8km away from the previous spot. As this chemical is not volatile, it does not evaporate and its mass is roughly conserved into the system until its natural decay acts. West Bay is much shallower than St Andrew Bay, thus the small concentration decrease close to the Gulf entrance involves a large pollutant mass transfer into West Bay (Fig. 11).

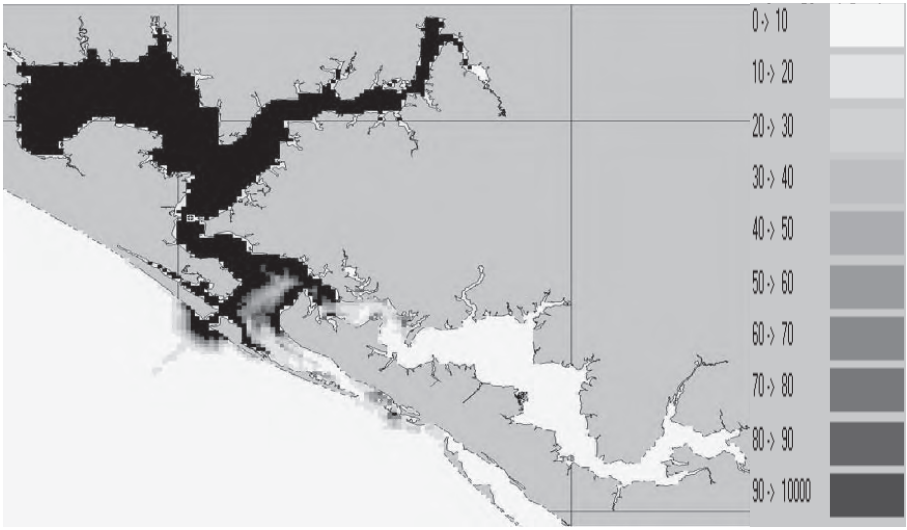

Fig. 11. Worst case maximum dissolved concentration (mg/m^3) with spill released at point A.

5.7. CONCLUSIONS

Because the chemical data embedded provided substances which were either immediately dissolved into water after their release, like ethylene glycol, or into the sediment, like tetraethyl lead, or even too volatile for remaining into the water, we could not study the differences implied by releases at surface and bottom. We plainly proved the furthest importance of the wind in the pollution drift, particularly in St Andrew Bay system where the shallowness gives an outstanding weight to the wind in driving the flow. Because the water flows inward at Gulf entrances and splits asymmetrically mostly towards West Bay, the dependence of the chemical dispersion on the release point is strong and East Bay is hardly impacted unless the pollution takes source in the bay itself or when winds are blowing eastward. The chemical clearly propagates westward during the simulation with a concentration generally damping away from the source except in very shallow zones where

some accumulation can occur with favorable winds. These accumulations are finally responsible of secondary pollution events. It is, at last, obvious that these results were biased, again, by the bathymetry smoothing process. However, it is reasonable to conclude that, as East Bay presents a rather uniform depth, this bias impact was not so crucial in this area and also that most of the pollution drift relied on the wind. Furthermore, the description of different salt diffusion processes during ebb and flood tides besides the observation that spring tides were globally causing a general freshening of the system by pumping fresh water while neap tides let salt to diffuse from the saltier St Andrew Bay towards both East Bay and particularly West Bay constituted two central resulting outcomes. The tidal impact study finally described an estuarine circulation with imbalanced ebb and flood periods.

ACKNOWLEDGMENTS

This work was funded by the Naval Oceanographic Office, the Office of Naval Research, and the Naval Postgraduate School.

REFERENCES

Atkinson,L.P., Lee, T.N., Blanton,J.O., and Chandler, W.S., 1983. Climatology of the southeastern United States continental shelf waters. Journal of Geophysical Research 88: 4705-4718.

Blumberg Alan F. and B. N. Kim, 2000. Flow balances in St. Andrew Bay revealed through hydrodynamic simulations. Estuaries 23(1): 21–33.

Chu, P.C., S. H. Lu, and Y. C. Chen, 2001. Evaluation of the Princeton Ocean Model using the South China Sea Monsoon Experiment (SCSMEX) Data. Journal of Atmospheric and Oceanic Technology 18: 1521-1539.

Chu, P.C., L.M. Ivanov, and O.M. Melnichenko, 2005a. Fall-winter current reversals on the Texas-Louisiana continental shelf. Journal of Physical Oceanography, 35, 902-910.

Chu, P.C., C.-L. Fang,and C.S. Kim, 2005b. Japan/East Sea model predictability. Continental Shelf Research, 25, 2107-2121.

Fischer H.B., List, E.J., Koh, R.C.Y., Imberger, J., and Brooks, N.H., 1979. Mixing in Inland and Coastal Waters. Academic Press, 483 pp, San Diego.

Jain, M., Mehta, A. J., van de Kreeke, J., and Dombrowski, M. R., 2004. Observations on the stability St. Andrew Bay inlets in Florida. Journal of Coastal Research 20 (3): 913-919.

McCay, F. D.P., and Isaji, T., 2004. Evaluation of the consequences of chemical spills using modeling: chemicals used in deepwater oil and gas operations. Environmental Modeling & Software 19(7-8): 629-644.

Muin, M., and Spaulding, M. L., 1996. Two-dimensional boundary fitted circulation model in spherical coordinates. Journal of Hydraulic Engineering 122 (9): 512-520.

Muin, M., and Spaulding, M. L., 1997. Three-dimensional boundary fitted circulation model. Journal of Hydraulic Engineering 123(1): 2-12.

Musgrove, R. H., Foster, J. B., and Toler, L. G., 1965. Water resources of the Ecofina Creek basin area in northwestern Florida. Report of Investigation No. 41. Florida Geological Survey. United States Geological Survey, Florida.

Pritchard, D. W., 1952. Estuarine hydrography. Advances in geophysics I. New York: Academic Press, pp. 243-280.

Roberts,H.H., McBride,R.A. and Coleman,J.M. (1999). Outer shelf and slope geology of the Gulf of Mexico: An overview. The Gulf of Mexico Large Marine Ecosystem (Kumpf,H., Steidinger,K. and Sherman,K., Eds.), pp. 93-112. Blackwell Science, Malden, MA.

Solis, R.S., and Powell, G.L., 1999. Hydrography, mixing characteristics, and residence times of Gulf of Mexico estuaries. Biogeochemistry of Gulf of Mexico Estuaries (Bianchi,T.S., Pennock,J.S. and Twilley,R.R., Eds.), pp. 29-61. John Wiley & Sons, Inc., New York.

Spaulding, M. L., Mendelsohn, D., and Swanson, J. C., 1999. WQMAP: An integrated three-dimensional hydrodynamic and water quality model system for estuarine and coastal applications. Marine Technology Society Journal, invited paper, Special issue on state of the art in ocean and coastal modeling 33(3): 38-54.

U. S. Army Corps of Engineers. National Shoreline Study - Regional Inventory Report. South Atlantic Division, Atlanta, Georgia, August 1971.

Weisberg, R.H., Z. Li, and Muller-Karger, F.E., 2001. West Florida shelf response to local wind forcing: April 1998. Journal of Geophysical Research 106: 31239-31262.

Wiseman,W.J.,Jr., and Sturges,W., 1999. Physical oceanography of the Gulf of Mexico: Processes that regulate its biology. The Gulf of Mexico Large Marine Ecosystem (Kumpf,H., Steidinger,K. and Sherman,K., Eds.), pp. 77-92. Blackwell Science, Malden, MA.